The Role of the Combustion Submodel for Large Eddy Simulation of Transient Premixed Flame-Vortex Interactions in Gas Explosions

Valeria Di Sarli*[a], Almerinda Di Benedetto[b], Gennaro Russo[b]

[a]Istituto di Ricerche sulla Combustione - Consiglio Nazionale delle Ricerche (IRC-CNR), Via Diocleziano 328, 80124, Napoli, Italy
[b]Dipartimento di Ingegneria Chimica, Università degli Studi Federico II, Piazzale Tecchio 80, 80125, Napoli, Italy
valeria.disarli@irc.cnr.it

In this paper, the sensitivity of large eddy simulation (LES) to the presence of the combustion submodel was investigated for transient interactions between premixed flame fronts and toroidal vortex structures generated at the wake of a circular orifice. To this end, LES computations were run, with and without the combustion submodel, for two orifice diameters: 40 mm and 20 mm. Nonuniform unstructured grids with a cell characteristic length varying in the range of 0.5-1 mm were used. In going from the 40-mm orifice to the 20-mm orifice, both the size and velocity of the vortex increase, leading to a different regime of interaction with the flame: the vortex only wrinkles the flame front in the 40-mm case (wrinkled regime) and also disrupts the continuity of the front, giving rise to the formation of separate reaction zones (i.e., flame pockets that leave the main front), in the 20-mm case (breakthrough regime). It has been found that the impact of the combustion submodel on LES predictions is strongly dependent on the regime of interaction. Results for the 40-mm orifice are substantially the same, regardless of the presence of the combustion submodel. Conversely, at the wake of the 20-mm orifice, the intensity of the flame-vortex interaction is such that the combustion submodel is strictly needed to reproduce both the qualitative (evolution of the pockets formed and their interaction with the main front) and quantitative (flame speed) characteristics of the flame propagation correctly.

1. Introduction

Turbulent premixed flames, both steady and unsteady, are involved in several engineering applications (gas turbine combustors, industrial burners, spark ignition engines, boilers, furnaces, etc.). Such flames are also found in gas and vapor cloud explosions that represent a major issue for chemical and process industries.

In practical situations, when an explosion occurs, the flame propagating away from an ignition source encounters obstacles (vessels, pipes, tanks, walls, flow cross-section variations, instrumentation, etc.) along its path. The unsteady coupling of the moving flame and the flow field induced by the presence of local blockage produces vortex structures of different length and velocity scales ahead of the flame front. The flame-vortex interaction leads the initially laminar flame to burn through various turbulent combustion regimes, which are dependent on both the size and velocity of the vortices encountered, thus accelerating the flame and increasing the rate of pressure rise (Di Sarli et al., 2007).

In order to understand and control the hazards and risks associated with gas and vapor cloud explosions, predictive computational fluid dynamics (CFD) models are required (Di Benedetto and Di Sarli, 2010).

Over the past decade, the rapid increase in computing power has led to considerable progress in the development of CFD techniques based on large eddy simulation (LES) for modeling turbulent reacting flows. LES is replacing classical (and less computationally demanding) methods based on Reynolds averaging (i.e., RANS methods) for its ability to provide a better representation of turbulence and, thus, the resulting flame-turbulence interaction. LES grasps the inherently time-dependent nature of turbulent flows and, therefore, is particularly fit for simulating transient combustion phenomena such as flame propagation during the course of explosions. This is confirmed in several literature works (Masri et al., 2006; Di Sarli et al., 2009a; 2009b; 2010; Gubba et al., 2009).

LES directly resolves the large vortex structures in a flow field, from the length scale of the computational domain down to a cutoff length scale linked to the grid cell size, and only models the subgrid structures (that, however, exhibit a more universal behavior). The grid resolution represents the scale separation between the length scales of computed (resolved) turbulence and those of modeled (unresolved) turbulence. As the grid size decreases, the unresolved contribution decreases up to the point of reaching the asymptote of direct numerical simulation (DNS), with all turbulent scales computed and no need for subgrid turbulence models (Pope, 2004).

LES of turbulent reacting flows also needs a combustion submodel (Poinsot and Veynante, 2005; Pitsch, 2006). Indeed, LES does not resolve the flame on the computational grid (the premixed flame thickness is smaller than the grid size used). Consequently, the flame and its interaction with the subgrid vortices have to be modeled, whereas the effects of the large vortices on the flame propagation are explicitly resolved.

Recently, we investigated the effect of the grid resolution on the impact of the combustion submodel for LES of transient premixed flame-vortex interactions in gas explosions (Di Sarli et al., 2012). To this end, LES computations were run, with and without the combustion submodel, on three nonuniform grids with a cell characteristic length (Δ) varying in the ranges of 2-3 mm, 1-2 mm and 0.5-1 mm. Numerical predictions were compared to the experimental data acquired by Long et al. (2006) during the interaction of a propagating flame front with a toroidal vortex generated at the wake of a circular orifice. Experiments were conducted by changing the orifice diameter, which directly controls the size and velocity of the vortex, from 40 mm to 30 and 20 mm (Long et al., 2006). LES calculations were performed for the 30-mm orifice. For this orifice size, results show that the solution obtained with the finer grid (having a resolution of the same order of magnitude as the laminar flame thickness) is independent of the presence of the combustion submodel. Indeed, the amount of detail explicitly resolved by LES is such that, even without using any combustion submodel, the predictions calculated with this grid correctly match the experimental data, in both quantitative (flame speed and flow velocity) and qualitative (shape and structure of the flame front) terms.

In this paper, our previous investigation was extended to the cases of the 40- and 20-mm orifices. The sensitivity of LES to the presence of the combustion submodel was thus quantified for different vortex sizes and velocities (i.e., different combustion regimes). Three-dimensional nonuniform unstructured grids with Δ = 0.5-1 mm were used.

2. Large Eddy Simulation (LES) model

The LES model of unsteady premixed flame propagation used in this work has been described and validated previously (Di Sarli et al., 2009a; 2010; 2012). Briefly, the model equations were obtained by filtering the governing equations for unsteady compressible flows with premixed combustion, i.e., the reactive Navier-Stokes equations for conservation of mass, momentum, energy and chemical species, joined to the constitutive and state equations. The species balance equation was recast in the form of a transport equation for the reaction progress variable, c ($c = 0$ within fresh reactants and $c = 1$ within burned products) (Libby and Williams, 1994).

To filter the governing equations, a low-pass box filter in the physical space (Poinsot and Veynante, 2005) was used. The filter width (Δ) was equal to the cubic root of the grid cell volume (i.e., equal to the characteristic length of the grid cell).

The filtering operation filters out the turbulent structures with length scales smaller than the filter width. Thus, the resulting equations govern the dynamics of the large-scale structures. However, because of the nonlinear nature of the conservation equations, the filtering process gives rise to unknown subgrid scale (SGS) terms that have to be modeled (Poinsot and Veynante, 2005).

The unknown terms arising from the filtering operation applied to the momentum equation and the energy equation are the SGS stress tensor and the sgs heat flux, respectively. The LES Favre-filtered (i.e., mass-weighted filtered) c-equation was written as follows:

$$\frac{\partial \overline{\rho} \tilde{c}}{\partial t} + \nabla \cdot \left(\overline{\rho} \tilde{u} \tilde{c} \right) + \nabla \cdot \left[\overline{\rho} \left(uc - \tilde{u} \tilde{c} \right) \right] = \overline{\nabla \cdot \left(\rho D \nabla c \right)} + \overline{\dot{\omega}_c}$$

(1)

where the overbar (—) denotes a filtered quantity and the tilde (~) denotes a Favre-filtered quantity. In Eq. 1, the (three) unknown terms are the SGS reaction progress variable flux (third term on the left-hand side), the filtered molecular diffusion (first term on the right-hand side) and the SGS reaction rate (second term on the right-hand side).

The SGS stress tensor was described using the dynamic Smagorinsky-Lilly eddy viscosity model (Lilly, 1992). The closure for the SGS fluxes of heat and reaction progress variable was achieved through the gradient hypothesis along with the SGS turbulent Prandtl and Schmidt numbers (Poinsot and Veynante, 2005).

To handle the flame-turbulence interaction, the Flame Surface Density (FSD) formalism was used (Poinsot and Veynante, 2005). Accordingly, the two right-hand side terms in Eq. 1 (i.e., the filtered terms of molecular diffusion and reaction rate) were included in a single flame front displacement term, $\overline{\rho w |\nabla c|}$, which was expressed as

$$\overline{\rho w |\nabla c|} = \overline{\nabla \cdot \left(\rho D \nabla c \right)} + \overline{\dot{\omega}_c} = \langle \rho w \rangle_S \Sigma$$

(2)

where Σ is the SGS flame surface density (i.e., the SGS flame surface per unit volume) and $\langle \rho w \rangle_s$ is the surface-averaged mass-weighted displacement speed, which was approximated by the product of the fresh gas density (ρ_0) and the laminar burning velocity (S_L) (Trouvé and Poinsot, 1994). Σ was expressed as a function of the SGS flame wrinkling factor, Ξ_Δ, (i.e., the SGS flame surface divided by its projection in the propagating direction), which takes into account the coupling of flame propagation and unresolved turbulence:

$$\overline{\rho w |\nabla c|} = \langle \rho w \rangle_S \Sigma = \rho_0 S_L \Xi_\Delta |\nabla \overline{c}|$$

(3)

Ξ_Δ in Eq. 3 was modeled according to the SGS combustion closure by Charlette et al. (2002). Such a closure is essentially a flame wrinkling model that, however, also works well beyond the wrinkled regime of combustion (Charlette et al., 2002; Di Sarli et al., 2009a).

In order to quantify the sensitivity of LES to the presence of the SGS combustion model, computations were also run by setting $\Xi_\Delta = 1$ in Eq. 3 (i.e., without the SGS combustion model).

3. Configuration and conditions

LES computations were run for the experiments carried out by Long et al. (2006), using the test rig schematized in Figure 1a. Within this rig, a quiescent premixed charge of stoichiometric methane and air was ignited inside a small cylindrical prechamber (length = 35 mm, diameter = 70 mm) linked to the main chamber (150 mm x 150 mm x 150 mm) via a small orifice (length of 30 mm; variable diameter). The bottom end of the prechamber was fully closed. The upper end of the main chamber was sealed by a thin PVC membrane that ruptured soon after ignition, allowing the exhaust gases to escape.

Ignition was provided at the center of the bottom end of the prechamber. After ignition, the flame propagated through the prechamber, pushing unburned charge ahead of the flame front through the orifice. This motion of the reactants through the constriction resulted in a toroidal vortex being shed into the main chamber. As the flame continued to propagate through the charge, it interacted with the vortex structure, distorting the flame and altering its burning velocity. Figure 1b shows a two-dimensional sketch of the flame-vortex interaction (the toroidal vortex was schematized as a vortex pair).
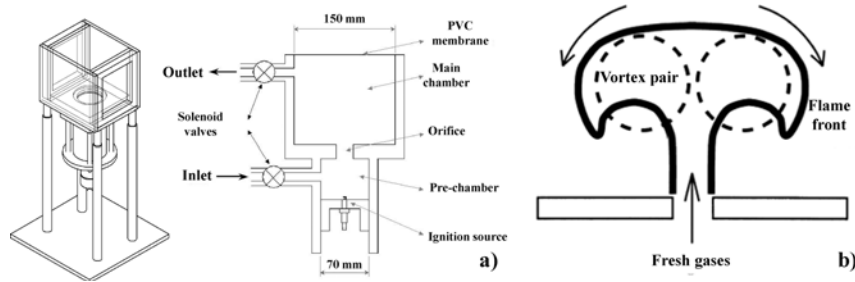

Figure 1: Schematic representations of (a) the test rig by Long et al. (2006) (not to scale) and (b) the flame-vortex interaction.

The nature (i.e., size and velocity) of the vortices produced in the main chamber is strongly dependent on the orifice diameter (Long et al., 2006). In this work, large eddy simulations were performed for two different orifice diameters: 40 mm and 20 mm.

4. Results and discussion

The manner in which a premixed flame front propagates through a turbulent flow field and, thus, the combustion regime experienced by the flame are strictly dependent on the size and velocity (i.e., strength) of the vortex structures encountered. In going from the 40-mm orifice to the 20-mm orifice, both these parameters increase, leading to a different regime of interaction with the flame. In order to quantify the combustion regimes for both orifices, we used the spectral diagram of flame-vortex interaction recently presented by Vasudeo et al. (2010). Consistently with the evolution of the structure of the propagating flame front, we have found that the flame-vortex interaction occurs inside the wrinkled regime for the 40-mm orifice and inside the breakthrough regime for the 20-mm orifice. In the wrinkled regime, the vortex only wrinkles the flame front. In the breakthrough regime, the interaction becomes stronger and the vortex also disrupts the continuity of the front, giving rise to the formation of flame pockets (i.e., separate reaction zones) that leave the main front.

Figures 2 and 3 show the time sequences of the instantaneous LES maps of the SGS reaction rate, $\rho_0 \, S_L \, \Xi_\Delta \, |\nabla \overline{c}|$, obtained during the flame-vortex interaction at the wake of the 40-mm (Figure 2) and 20-mm (Figure 3) orifices, using the SGS combustion model by Charlette et al. (2002) (Figures 2a and 3a) and without the SGS combustion model (Figures 2b and 3b).
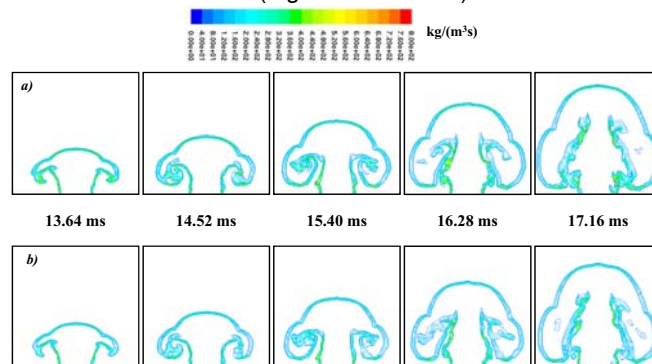

Figure 2: Time sequence of the instantaneous LES maps of the SGS reaction rate obtained (a) with and (b) without the SGS combustion model: 40-mm orifice.
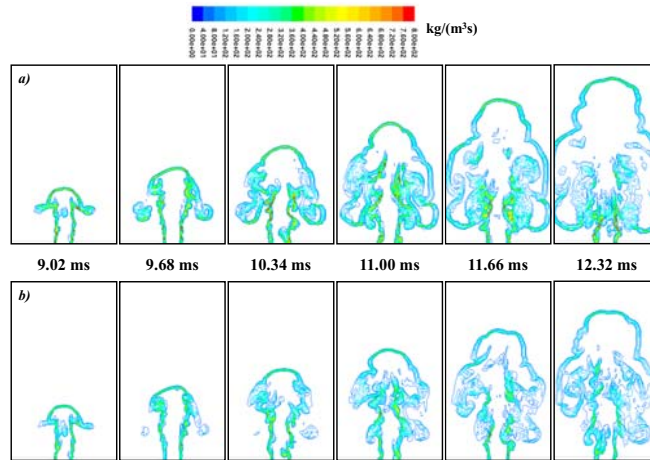
Figure 3: Time sequence of the instantaneous LES maps of the SGS reaction rate obtained (a) with and (b) without the SGS combustion model: 20-mm orifice.

The maps were taken along a vertical section through the computational domain, the plane of which was aligned to the central axis of the main chamber (i.e., the central section). In Figure 4, the flame speed is plotted versus the axial distance from the ignition face as obtained, for both orifices, from LES computations run with and without the SGS combustion model. The flame speed was evaluated from the displacement of the maximum downstream location of the flame front. The black rectangle along the x-axis indicates the position of the exit section of the orifice (65 mm).

Global assessment of Figures 2-4 shows that the impact of the SGS combustion model is strongly dependent on the regime of interaction. Regardless of the presence of the SGS combustion model, results for the 40-mm orifice (wrinkled regime) are substantially the same in both qualitative (shape and structure of the flame front) and quantitative (reaction rate and flame speed) terms. Indeed, for this orifice size, most of the interaction is resolved on the computational grid. Conversely, for the 20-mm orifice (breakthrough regime), strong differences can be observed between the predictions obtained with and without the SGS combustion model. The differences are not only quantitative, but also qualitative. In the absence of the SGS combustion model, the lower reaction rate compromises the capability of the pockets formed to grow and merge with the main flame front, thus sustaining its development. Unrealistic quenching phenomena are indeed observed for such pockets, which cause slower flame propagation. This highlights the need to take into account the SGS flame-turbulence interaction in the LES model to reproduce the flame propagation in the breakthrough regime (i.e., in a more intense turbulent combustion regime) correctly.
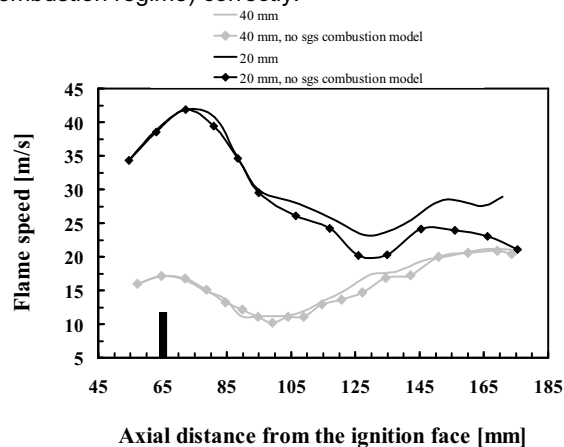

Figure 4: Flame speed versus the axial distance from the ignition face as obtained from LES computations run with and without the SGS combustion model: 40-mm and 20-mm orifices.

5. Conclusions

The continuously growing power of parallel computers will enable large eddy simulations of turbulent premixed combustion to be performed with fine grid resolution (of the order of the laminar flame thickness), such as that used in the present work, also at geometry scales larger than laboratory scales. In view of this, the main implication of the results obtained here is that LES modeling efforts should be focused on the development of combustion closures able to catch the transition through more intense regimes of premixed flame-vortex interaction than the wrinkled regime for which LES can be seen as a tool of direct simulation.

References

Charlette F., Meneveau C., Veynante D., 2002, A power-law flame wrinkling model for LES of premixed turbulent combustion Part I: Non-dynamic formulation and initial tests, Combust. Flame 131, 159-180.

Di Benedetto A., Di Sarli V., 2010, Theory, modeling and computation of gas explosion phenomena. In Handbook of Combustion, Vol. 3: Gaseous and Liquid Fuels; Lackner M., Winter F., Agarwal A.K., Eds., Wiley-VCH Verlag GmbH & Co. KGaA: Weinheim, Germany, 49-74.

Di Sarli V., Di Benedetto A., Salzano E., Ferrara G., Russo G., 2007, Mitigation of gas explosions in industrial equipment by means of venting systems. In New Research on Hazardous Materials; Warey P.B., Ed., Nova Science Publishers: New York, 249-291.

Di Sarli V., Di Benedetto A., Russo G., Jarvis S., Long E.J., Hargrave G.K., 2009a, Large eddy simulation and PIV measurements of unsteady premixed flames accelerated by obstacles, Flow Turbul. Combust. 83, 227-250.

Di Sarli V., Di Benedetto A., Russo G., 2009b, Using Large eddy simulation for understanding vented gas explosions in the presence of obstacles, J. Hazard. Mater. 169, 435-442.

Di Sarli V., Di Benedetto A., Russo G., 2010, Sub-grid scale combustion models for large eddy simulation of unsteady premixed flame propagation around obstacles, J. Hazard. Mater. 180, 71-78.

Di Sarli V., Di Benedetto A., Russo G., 2012, Large Eddy Simulation of transient premixed flame-vortex interactions in gas explosions, Chem. Eng. Sci. 71, 539-551.

Gubba S.R., Ibrahim S.S., Malalasekera W., Masri A.R., 2009, An assessment of large eddy simulations of premixed flames propagating past repeated obstacles, Combust. Theory Model. 13, 513-540.

Libby P.A., Williams F.A., Eds., 1994, Turbulent Reacting Flows; Academic Press: London.

Lilly D.K., 1992, A proposed modification of the Germano subgrid-scale closure method, Phys. Fluids A 4, 633-635.

Long E.J., Hargrave G.K., Jarvis S., Justham T., Halliwell N.J., 2006, Characterisation of the interaction between toroidal vortex structures and flame front propagation, J. Phys. Conf. Ser. 45, 104-111.

Masri A.R., Ibrahim S.S., Cadwallader B.J., 2006, Measurements and large eddy simulation of propagating premixed flames, Exp. Therm. Fluid Sci. 30, 687-702.

Pitsch H., 2006, Large-eddy simulation of turbulent combustion, Annu. Rev. Fluid Mech. 38, 453-482.

Poinsot T., Veynante D., 2005, Theoretical and Numerical Combustion, Second Edition; R.T. Edwards: Philadelphia, PA.

Pope S.B., 2004, Ten questions concerning the large-eddy simulation of turbulent flows, New J. Phys. 6, 1-35.

Trouvé A., Poinsot T., 1994, The evolution equation for the flame surface density in turbulent premixed combustion, J. Fluid Mech. 278, 1-31.

Vasudeo N., Echekki T., Day M.S., Bell J.B., 2010, The regime diagram for premixed flame kernel-vortex interactions Revisited, Phys. Fluids 22, 043602.